# Single quark transition model analysis of electromagnetic nucleon resonance excitations in the $[70,\ 1^-]$ supermultiplet

V. D. Burkert
*Thomas Jefferson National Accelerator Laboratory, Newport News, Virginia 23606*

R. De Vita, M. Battaglieri, and M. Ripani
*Istituto Nazionale di Fisica Nucleare, Sezione di Genova, 16146 Genova, Italy*

V. Mokeev
*Moscow State University, 119899 Moscow, Russia*
*and Christopher Newport University, Newport News, Virginia 23602*

(Received 14 August 2002; published 18 March 2003)

We apply the single quark transition model to resonance transition amplitudes extracted from photoproduction and electroproduction data. We use experimental data on the $S_{11}(1535)$ and $D_{13}(1520)$ nucleon resonances to extract the amplitudes for the electromagnetic transition from the nucleon ground state $[56,\ 0^+]$ to the $[70,\ 1^-]$ supermultiplet, and make predictions for the transition amplitudes of all other states associated with the $[70,\ 1^-]$. We compare the predictions with data and find surprisingly good agreement. The comparison is hampered by the poor data quality for many of the states especially in the electroproduction sector.

DOI: 10.1103/PhysRevC.67.035204 PACS number(s): 13.60.Le, 13.88.+e, 14.4.0Aq

## I. INTRODUCTION

Resonance excitation of protons and neutrons is a fundamental phenomenon of strong QCD. Descriptions of resonance excitations have made use of a broad range of constituent quark models to describe the excitation of *s*-channel baryon resonances. These models are often based on approximate $SU(6)\otimes O(3)$ symmetry for the spin-flavor and orbital excitations. This symmetry is broken by introducing additional interactions such as the one-gluon exchange [1] or Goldstone boson exchange between the constituent quarks [2], leading to the breaking of mass degeneracies between states belonging to the same supermultiplet $[SU(6),L^P]$, where $L^P$ characterizes the orbital angular momentum $L$ and parity $P$ of the three-quark system. The effects of symmetry breaking on the masses are typically $O(150\ \mathrm{MeV})$.

The early successes of the non-relativistic constituent quark model in approximately describing many aspects of hadron properties, as well as of nucleon structure, led to a broad application in electromagnetic interaction. Much effort has gone into describing resonance transition amplitudes and form factors [3]. While a reasonable description of many photocoupling amplitudes of low mass states has been achieved, with the Roper resonance $P_{11}(1440)$ being a notable exception, a persistent problem in these calculations is the description of the $Q^2$ evolution of the transition form factors based on quarks with pointlike couplings. This reflects our lack of a full understanding of the concept of constituent quarks versus the distance scale probed. Some progress has been made in recent years by introducing phenomenological form factors for the constituent quarks [4], and by going beyond the simple harmonic oscillator potential [5]. A promising approach has been taken recently in employing the field correlator method in calculating nonperturbative quark dynamics in baryons [6]. In this approach, constituent quark masses are generated dynamically.

In the approximation that only a single quark is affected in the transition [single quark transition model (SQTM)], simple relationships can be derived for excitations from the ground state nucleon to states assigned to the same $[SU(6),L^P]$ supermultiplet of the $SU(6)\otimes O(3)$ symmetry group [7–9]. Knowledge of only a few amplitudes from states within the same supermultiplet allows predictions of amplitudes for all other states within the same supermultiplet. In this analysis we will assume factorization of the spin and spatial transition matrix elements. $SU(6)\otimes O(3)$ symmetry breaking is accommodated by introducing mixing angles for states with the same spin, parity, and flavor, but different quark spins $S_{3q}=1/2,3/2$. We use previously determined mixing angles from the analysis of hadronic decay properties [23,24]. Resonance photocoupling amplitudes and their $Q^2$ dependences, including their signs, have been determined in analyses of pion photoproduction and electroproduction experiments taking into account the hadronic couplings as extracted from the analyses of hadronic resonance production. We use the signs as published which, by convention, are fixed relative to the pion Born amplitudes that are included in the analyses aimed at extracting resonance photocouplings. Analysis of these amplitudes within the SQTM provides information on the consistency of the ingredients obtained from hadronic interactions such as the mixing angle. The adopted mixing angles can be further tested using the $Q^2$ dependence of the amplitudes for the transition to the $S_{11}(1650)$ and $D_{13}(1700)$ states. Deviations from the predicted $Q^2$ dependences may indicate possible violations of the SQTM assumptions. $SU(6)$ symmetry and the single quark transition assumption may be further tested with the predictions for other states in the $[70,\ 1^-]$ supermultiplet.

Experimentally, electromagnetic excitation of nucleon resonances (we use nucleon resonances here for both isospin

 

1/2 and isospin 3/2 nonstrange baryons), have been studied mostly using single pion or eta production. With the new and precise photoproduction data which have been collected at MAMI [10]and GRAAL [11], and with the new photoproduction and electroproduction data from JLab [12–17], this field is seeing a vast improvement in data volume and precision, and much more is expected in various reaction channels for the near future. It is therefore timely to revisit some of the earlier attempts at coming to a more quantitative understanding of electromagnetic resonance excitations.

This paper is organized as follows. In Sec. II we define kinematical quantities and the formalism. In Sec. III we briefly review the single quark transition model assumptions and summarize the model predictions. In Sec. IV we review the existing photoproduction and electroproduction data. In Sec. V we present predictions for the transition amplitudes to the $[70,\ 1^-]_1$ supermultiplet and compare with the available data. Finally we discuss the results in Sec. VI.

## II. FORMALISM

The inclusive electron scattering cross section is given by

$$\frac{1}{\Gamma_T}\frac{d\sigma}{d\Omega dE'}=\frac{1}{2}(\sigma_T^{1/2}+\sigma_T^{3/2})+\epsilon_L\sigma_L, \tag{1}$$

where $\Gamma_T$ is the virtual photon flux, $\epsilon_L$ describes the degree of longitudinal polarization of the photon, $\sigma_T^{1/2}$ is the total transverse absorption cross section with helicity 1/2 for the photon-nucleon system, and $\sigma_T^{3/2}$ is the helicity 3/2 cross section. $\sigma_L$ is the total cross section for the absorption of a longitudinal photon. In the following we will focus on the transverse part of the cross section as there are insufficient data available for a systematic study of the longitudinal couplings of nucleon resonances.

In the nucleon resonance region it is convenient to expand the cross section for a specific production channel in terms of partial wave helicity elements. For example, in single pion photoproduction $\gamma p\rightarrow\pi N$ these are given by

$$\sigma_T^{1/2}=\frac{8\pi q}{k}\sum_{n=0}^{\infty}(n+1)(|A_{n+}|^2+|A_{n+1,-}|^2), \tag{2}$$

$$\sigma_T^{3/2}=\frac{8\pi q}{k}\sum_{n=0}^{\infty}\frac{1}{4}[n(n+1)(n+2)](|B_{n+}|^2+|B_{n+1,-}|^2),$$

where $q$ and $k$ are, respectively, the pion and photon center-of-mass momenta calculated at $Q^2=0$,

$$k=\frac{W^2-M^2}{2W}, \tag{3}$$

and

$$q=\sqrt{\frac{[W^2-(m_\pi^2-M^2)]-4W^2m_\pi^2}{2W}}, \tag{4}$$

and $A_{l\pm}$ and $B_{l\pm}$, with $(l=n,\ n+1)$, are the transverse partial wave helicity elements for the pion orbital angular momentum $l$ and helicity $\frac{1}{2}$ and $\frac{3}{2}$, respectively. The $l\pm$ indicates if the total resonance spin is given by $J=l\pm\frac{1}{2}$, $\pm\frac{1}{2}$ being the nucleon helicity in the initial state. These elements are extracted from the experimental data using partial wave analysis techniques.

TABLE I. CG coefficients.

| $I$ | $\pi^+n$ | $\pi^0p$ |
|---|---|---|
| $\frac{1}{2}$ | $-\sqrt{\frac{2}{3}}$ | $+\sqrt{\frac{1}{3}}$ |
| $\frac{3}{2}$ | $-\sqrt{\frac{1}{3}}$ | $-\sqrt{\frac{2}{3}}$ |

For a specific resonance the transverse total photoabsorption cross section can be expressed as a function of the transverse photocoupling helicity amplitudes

$$\sigma_T^{\rm res}=\frac{2M}{W_R\Gamma}\frac{1}{2}(A_{1/2}^2+A_{3/2}^2), \tag{5}$$

where $W_R$ is the resonance mass, and $\Gamma$ the total width.

The $A_{1/2}$, $A_{3/2}$ are related to the partial wave helicity elements in the following way:

$$A_{l\pm}=\mp fC_{\pi N}^I A_{1/2}, \tag{6}$$

$$B_{l\pm}=\pm f\sqrt{\frac{16}{(2j-1)(2j+3)}}C_{\pi N}^I A_{3/2},$$

where

$$f=\sqrt{\frac{1}{(2j+1)\pi}\frac{k}{q}\frac{M}{W_R}\frac{\Gamma_\pi}{\Gamma^2}}. \tag{7}$$

$C_{\pi N}^I$ are Clebsch-Gordan (CG) coefficients describing the projection of a resonant state of isospin $I$ into the final state $\pi N$ (see Table I). The $A_{l\pm}$, $B_{l\pm}$ can be determined directly from experimental data. Using information from hadronic reactions, the photocoupling helicity amplitudes $A_{1/2}$ and $A_{3/2}$ can then be determined. In the following sections we will use these amplitudes to describe the resonance transition to specific states, and give the connection to the SQTM amplitudes.

## III. SINGLE QUARK TRANSITION MODEL

Properties of nucleon resonances such as mass, spin-parity, and flavor fit well into the representation of the SU(6)⊗O(3) symmetry group, which describes the spin-flavor and orbital wave functions of the three-quark system [9]. This symmetry group leads to supermultiplets of baryon states with the same orbital angular momentum $L$ of the three-quark system and degenerate energy levels. Within a supermultiplet the quark spins are aligned to form a total quark spin $S=\frac{1}{2}$, $\frac{3}{2}$, which combines with the orbital angular momentum $L$ to the total angular momentum. A large number of explicit dynamical quark models have been developed to describe the electromagnetic transition between the nucleon ground state and its excited states [5,18,19]. Mea-

surement of resonance transitions and the dependence on the distance scales, given by the virtuality $Q^2$ of the photon, provides information on the nucleon wave function. In order to compute the transition, assumptions on the three-quark potential and the quark-quark interactions have to be made. These are then tested by predicting photocoupling helicity amplitudes which can then be confronted with experimental data.

In this paper we use algebraic relations derived in the literature for resonance transitions assuming the transition only affects a single quark in the nucleon. The parameters in these algebraic equations are then determined from experimental analysis. Based on the symmetry properties of the SQTM, predictions for a large number of resonance transitions can then be made.

The fundamentals of the SQTM have been described in references [7,8], where the symmetry properties have been discussed for the transition from the ground state nucleon $[56,\ 0^+]$ to the $[70,\ 1^-]$ and the $[56,\ 2^+]$ supermultiplets. The $[70,\ 1^-]$ contains states which are prominent in electromagnetic excitations, and it is the only supermultiplet for which sufficient data on resonance couplings of two states are available to extract the SQTM amplitudes and test predictions for other states.

The coupling of the electromagnetic current is considered for the transverse photon component, and the quarks in the nucleon are assumed to interact freely with the photon. It has been discussed extensively in the literature [7–9] that in such a model the quark transverse current can be written in general as a sum of four terms

$$J^+ = AL^+ + B\sigma^+ L_z + C\sigma_z L^+ + D\sigma^- L^+ L^+, \tag{8}$$

where $\sigma$ is the quark Pauli spin operator, and the terms with $A$, $B$, $C$, $D$ in front operate on the quark spatial wave function changing the component of orbital angular momentum along the direction of the momentum transfer ($z$ axis). The $A$ term corresponds to a quark orbit flip with $\Delta L_z = +1$, term $B$ to a quark spin flip with $\Delta L_z = 0$, the $C$ and $D$ terms correspond to simultaneous quark orbit and quark spin flip with orbital angular momentum flips of $\Delta L_z = +1$ and $\Delta L_z = +2$, respectively. For the transition from the $[56,\ 0^+]$ to the $[70,\ 1^-]$ supermultiplet with $L=1$, only $A$, $B$, and $C$ are allowed. We limit our discussion to the $[70,\ 1^-]$ supermultiplet as there is currently insufficient experimental information available to extract the SQTM amplitudes for transitions to other supermultiplets.

For the simplest nonrelativistic constituent quark model [20,21], only the orbit flip ($A$) and spin flip ($B$) operators are nonzero, showing the incompleteness of these descriptions. The algebraic relations for resonance transitions derived from symmetry properties of the SQTM are given in Sec. V. Knowledge of three amplitudes and of two mixing angles for the transition to the $[70,\ 1^-]$ allows predictions for 16 amplitudes of states belonging to the same supermultiplet. If they can be confirmed for some of the amplitudes, we have a measure of the degree to which electromagnetic transitions of nucleon resonance are dominated by single quark transitions at the photon point ($Q^2=0$) and, using electroproduction data, examine if and how this is changing as a function of the distance scale at increasing photon virtuality.

To present the experimental data we will use the quark electric and magnetic multipoles of Cottingham and Dunbar [7]. They provide direct physical insight into the resonance transition, and also allow simple parametrizations. The $A$, $B$, $C$ are simply linear combinations of the quark multipoles. For the $[70,\ 1^-]$ multiplet these relations are given by

$$\begin{aligned} A &= K \times 2\sqrt{3} e^{11}, \\ B &= -K \times (\sqrt{6} m^{11} - \sqrt{6} m^{12}), \\ C &= K \times (\sqrt{6} m^{11} + \sqrt{6} m^{12}), \end{aligned} \tag{9}$$

where

$$K = \frac{e}{2} \frac{1}{\sqrt{M(W^2 - M^2)}}. \tag{10}$$

Similar relations have been derived for the transition from the ground state $[56,\ 0^+]$ to the $[56,\ 2^+]$ supermultiplet. In this case all four SQTM amplitudes contribute which, due to the lack of data, currently cannot be determined unambiguously. We will, therefore, not discuss the transitions to that multiplet here. However, new data from JLab, covering a more limited $Q^2$ range in two-pion electroproduction [17], may allow determination of several states in $[56,\ 2^+]$ in the future.

*Violation of SU(6) selection rules*. SU(6) symmetry results in selection rules for transitions to some of the states in the $[70,\ 1^-]$ multiplet. For example, electromagnetic transitions from proton targets to states in the $N^4$ quadruplet with quark spin $\frac{3}{2}$ are not allowed by the Moorhouse selection rule [22]. SU(6) symmetry is, however, broken due to configuration mixing between various baryon states. Mixing is naturally explained as a results of color hyperfine interaction between quarks [1] or due to Goldstone boson exchanges [2]. We take these effects into account in the usual way by introducing mixing angles for two of the configurations associated with the $[70,\ 1^-]$ multiplet. Mixing is present for the $N^2$ and the $N^4$ nucleon states. The $\frac{1}{2}^-$ states are mixed with an angle of $\approx 31°$, estimated from hadronic decay properties [23,24], leading to the physical states:

$$\begin{aligned} |S_{11}(1535)\rangle &= 0.85 \left| N^2, \frac{1}{2}^- \right\rangle - 0.53 \left| N^4, \frac{1}{2}^- \right\rangle, \\ |S_{11}(1650)\rangle &= 0.53 \left| N^2, \frac{1}{2}^- \right\rangle + 0.85 \left| N^4, \frac{1}{2}^- \right\rangle, \end{aligned} \tag{11}$$

where the $|N^2, \frac{1}{2}^-\rangle$ and $|N^4, \frac{1}{2}^-\rangle$ correspond to the nucleon doublet and quadruplet with quark spin $\frac{1}{2}$ and $\frac{3}{2}$, respectively. A much smaller mixing has been observed for the $|N^2, \frac{3}{2}^-\rangle$ and $|N^4, \frac{3}{2}^-\rangle$ states, with a mixing angle of $\approx 6°$, leading to

$$|D_{13}(1520)\rangle = 0.99\left|N^2,\frac{3}{2}^-\right\rangle - 0.11\left|N^4,\frac{3}{2}^-\right\rangle,$$
$$|D_{13}(1700)\rangle = 0.11\left|N^2,\frac{3}{2}^-\right\rangle + 0.99\left|N^4,\frac{3}{2}^-\right\rangle. \quad (12)$$

As mentioned above, in the SQTM $|N^4,\frac{1}{2}^-\rangle = |N^4,\frac{3}{2}^-\rangle = 0$ for proton targets. However, due to the large mixing angle for the $\frac{1}{2}^-$ states, the SQTM predicts a sizable excitation of the $S_{11}(1650)$, while the $D_{13}(1700)$ should only be weakly excited from proton target. The $D_{15}(1675)$ cannot mix with any other state, and thus cannot be excited from proton targets with the SQTM approach.

## IV. EXPERIMENTAL HELICITY AMPLITUDES

The test of the SQTM predictions was performed including all photoproduction data and all electroproduction data from proton targets presently available. We did not include electroproduction data from neutron targets as the data quality is too poor for a meaningful comparison with our prediction. The resonance helicity amplitudes at the photon point were taken from the Particle Data Group [25]. This compilation already combines the outcomes of various analyses, such as the ones of Refs. [26–29]. Electroproduction data on the helicity amplitudes are more sparse and available only for the most prominent states. In this analysis we included data from Bonn [30], DESY [31], NINA [32], and JLab [13,14]. A compilation of the results obtained at Bonn, DESY, and NINA for $\pi$ and $\eta$ electroproduction can be found in Ref. [33]. In addition to the outcomes of the original analysis, we also included the results obtained in the analysis of Ref. [34,35] and the results of the world data analysis on

TABLE II. Helicity amplitudes of the $[70,1^-]$ multiplet on a proton target as a function of the quark multipoles $e^{11}$, $m^{11}$, and $m^{12}$.

| State | Amplitude | $f^1$ | $f^2$ | $f^3$ |
|---|---|---|---|---|
| $S_{11}(1535)$ | $A_{1/2}$ | $\sqrt{\frac{1}{3}}\cos 31°$ | $-\sqrt{\frac{2}{3}}\cos 31°$ | |
| $D_{13}(1520)$ | $A_{1/2}$ | $\sqrt{\frac{1}{6}}\cos 6°$ | $\sqrt{\frac{1}{12}}\cos 6°$ | $-\sqrt{\frac{3}{4}}\cos 6°$ |
| | $A_{3/2}$ | $\sqrt{\frac{1}{2}}\cos 6°$ | $\frac{1}{2}\cos 6°$ | $\frac{1}{2}\cos 6°$ |
| $S_{11}(1650)$ | $A_{1/2}$ | $\sqrt{\frac{1}{3}}\sin 31°$ | $-\sqrt{\frac{2}{3}}\sin 31°$ | |
| $S_{31}(1620)$ | $A_{1/2}$ | $\sqrt{\frac{1}{3}}$ | $\sqrt{\frac{2}{27}}$ | |
| $D_{15}(1675)$ | $A_{1/2}$ | | | |
| | $A_{3/2}$ | | | |
| $D_{13}(1700)$ | $A_{1/2}$ | $\sqrt{\frac{1}{6}}\sin 6°$ | $\sqrt{\frac{1}{12}}\sin 6°$ | $-\sqrt{\frac{3}{4}}\sin 6°$ |
| | $A_{3/2}$ | $\sqrt{\frac{1}{2}}\sin 6°$ | $\frac{1}{2}\sin 6°$ | $\frac{1}{2}\sin 6°$ |
| $D_{33}(1700)$ | $A_{1/2}$ | $\sqrt{\frac{1}{6}}$ | $-\frac{1}{2\sqrt{27}}$ | $\sqrt{\frac{1}{12}}$ |
| | $A_{3/2}$ | $\sqrt{\frac{1}{2}}$ | $-\frac{1}{6}$ | $-\frac{1}{6}$ |

TABLE III. Helicity amplitudes of the $[70,1^-]$ multiplet on a neutron target as a function of the quark multipoles $e^{11}$, $m^{11}$, and $m^{12}$.

| State | Amplitude | $f^1$ | $f^2$ | $f^3$ |
|---|---|---|---|---|
| $S_{11}(1535)$ | $A_{1/2}$ | $-\sqrt{\frac{1}{3}}\cos 31°$ | $\sqrt{\frac{2}{27}}\cos 31° - \sqrt{\frac{2}{27}}\sin 31°$ | |
| $D_{13}(1520)$ | $A_{1/2}$ | $-\sqrt{\frac{1}{6}}\cos 6°$ | $-\frac{1}{2\sqrt{27}}\cos 6° + \frac{1}{2}\sqrt{\frac{10}{27}}\sin 6°$ | $\sqrt{\frac{1}{12}}\cos 6° + \sqrt{\frac{1}{30}}\sin 6°$ |
| | $A_{3/2}$ | $-\sqrt{\frac{1}{2}}\cos 6°$ | $-\frac{1}{6}\cos 6° + \frac{\sqrt{10}}{6}\sin 6°$ | $-\frac{1}{6}\cos 6° - \frac{1}{3}\frac{1}{\sqrt{10}}\sin 6°$ |
| $S_{11}(1650)$ | $A_{1/2}$ | $-\sqrt{\frac{1}{3}}\sin 31°$ | $\sqrt{\frac{2}{27}}\sin 31° - \sqrt{\frac{2}{27}}\cos 31°$ | |
| $S_{31}(1620)$ | $A_{1/2}$ | $\sqrt{\frac{1}{3}}$ | $\sqrt{\frac{2}{27}}$ | |
| $D_{15}(1675)$ | $A_{1/2}$ | | $-\frac{1}{2\sqrt{27}}$ | $-\sqrt{\frac{2}{15}}$ |
| | $A_{3/2}$ | | $-\frac{1}{6}$ | $-\sqrt{\frac{4}{15}}$ |
| $D_{13}(1700)$ | $A_{1/2}$ | $-\sqrt{\frac{1}{6}}\sin 6°$ | $-\frac{1}{2\sqrt{27}}\sin 6° - \frac{1}{2}\sqrt{\frac{10}{27}}\cos 6°$ | $\sqrt{\frac{1}{12}}\sin 6° - \sqrt{\frac{1}{30}}\cos 6°$ |
| | $A_{3/2}$ | $-\sqrt{\frac{1}{2}}\sin 6°$ | $-\frac{1}{6}\sin 6° - \frac{\sqrt{10}}{6}\cos 6°$ | $-\frac{1}{6}\sin 6° + \frac{1}{3}\frac{1}{\sqrt{10}}\cos 6°$ |
| $D_{33}(1700)$ | $A_{1/2}$ | $\sqrt{\frac{1}{6}}$ | $-\frac{1}{2\sqrt{27}}$ | $\sqrt{\frac{1}{12}}$ |
| | $A_{3/2}$ | $\sqrt{\frac{1}{2}}$ | $-\frac{1}{6}$ | $-\frac{1}{6}$ |

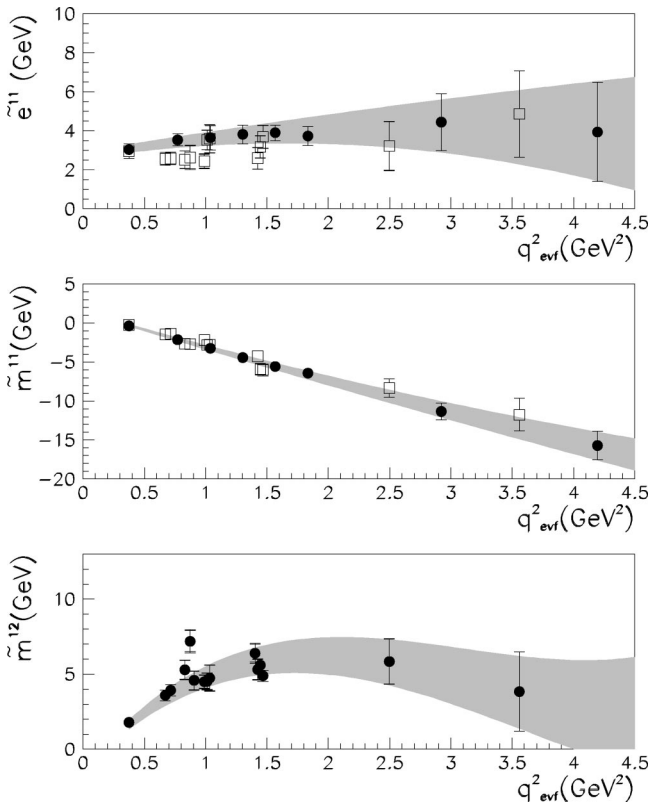


FIG. 1. Extracted quark multipoles as a function of the equal-velocity-frame momentum transfer for the $[70,\ 1^-]$ multiplet. The shaded band shows the fit results. Their width accounts for the uncertainty on the experimental points. In the first two graphs, the open squares have been obtained from the Bonn, NINA, and DESY data, while the full circles are based on the new JLab measurements. In the third plot, all the data are from the Bonn, NINA, and DESY measurements. Only the full points were used to derive the quark multipoles parametrization.

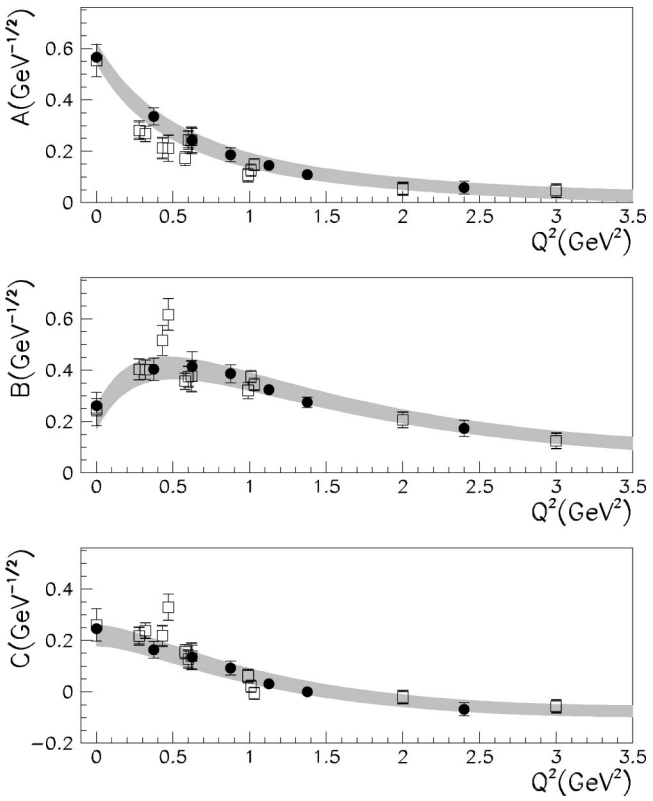


FIG. 2. Single quark transition amplitudes *A*, *B*, *C* for the $[70,\ 1^-]$ multiplet. The shaded band shows the result of the fit of the reduced quark multipoles. The width of the band accounts for the uncertainties of the experimental data.

$\eta$ electroproduction at the $S_{11}(1535)$ mass presented in Ref. [14].

### V. SQTM FIT FOR THE [70, 1$^-$] MULTIPLET

As discussed in Sec. III, the helicity amplitudes of all the states that belong to $[70,\ 1^-]$ multiplet can be expressed in terms of three SQTM amplitudes at fixed $Q^2$, and the mixing angles obtained from hadronic resonance decays. Therefore three experimentally measured amplitudes are sufficient to determine completely the transition from the ground state to this multiplet at fixed $Q^2$. For further analysis it is convenient to use the quark multipole moments $e^{11}$, $m^{11}$, and $m^{12}$ introduced in Ref. [7]. They provide direct physical insight and allow simple parametrizations. The relations between these quantities and the resonance helicities amplitudes can be written as

$$A_{\frac{1}{2},\frac{3}{2}} = K\left[ f^1_{\frac{1}{2},\frac{3}{2}} m^{12} + f^2_{\frac{1}{2},\frac{3}{2}} e^{11} + f^3_{\frac{1}{2},\frac{3}{2}} m^{11} \right]. \tag{13}$$

The coefficients $f^i_{1/2,3/2}$ for proton and neutron targets are summarized in Tables II and III.

To investigate the $Q^2$ dependence of the quark multipoles, the equal velocity frame (EVF) was chosen. In this frame the initial and final hadrons have equal and opposite velocities resulting in minimal relativistic corrections. The four-momentum transfer in the equal velocity frame can be written as

$$\mathbf{q}^2_{\mathrm{EVF}} = \frac{W^2 - M^2}{4WM} + Q^2 \frac{W^2 + M^2}{4WM}. \tag{14}$$

In order to allow for a simple parametrization of the quark multipoles we separate out a common form factor in the $Q^2$ dependence of the resonance excitation. We used the usual dipole form

$$F(\mathbf{q}^2_{\mathrm{EVF}}) = (1 + \mathbf{q}^2_{\mathrm{EVF}}/0.71)^{-2}. \tag{15}$$

The quark multipoles were then written as

$$\begin{aligned} e^{11} &= \tilde{e}^{11} F(\mathbf{q}^2_{\mathrm{EVF}}), \\ m^{11} &= \tilde{m}^{11} F(\mathbf{q}^2_{\mathrm{EVF}}), \\ m^{12} &= \tilde{m}^{12} F(\mathbf{q}^2_{\mathrm{EVF}}), \end{aligned} \tag{16}$$

where $\tilde{e}^{11}$, $\tilde{m}^{11}$, and $\tilde{m}^{12}$ are called reduced quark multipoles. The helicity amplitudes for the $S_{11}(1535)$ and

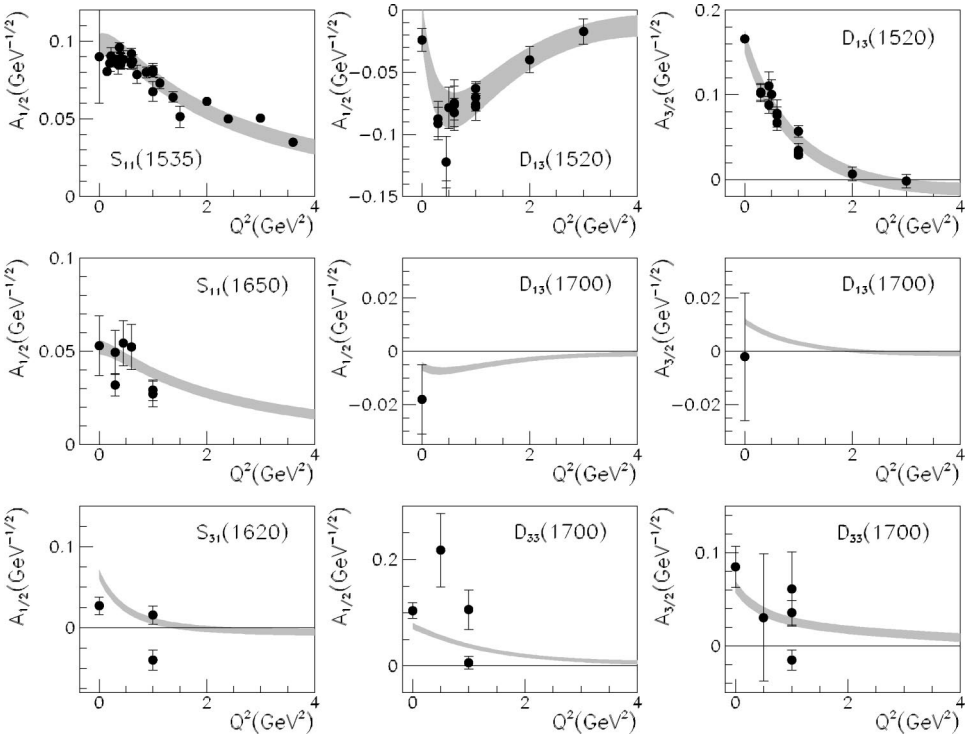


FIG. 3. Single quark model prediction for the [70, $1^-$] multiplet on the proton. The SQTM predictions are shown by the shaded band in comparison with the experimental data. At $Q^2=0$ the full circle is the Particle Data Group estimate. For $Q^2>0$, measurements from JLab, Bonn, DESY, and NINA in $\eta$ and $\pi$ electroproduction are shown. For the $S_{11}(1535)$, the results of an analysis of the world data in $\eta$ electroproduction presented in Ref. [14] are also included.

$D_{13}(1520)$ resonances, which are the best known states of the [70, $1^-$] multiplet, were used to derive the quark multipoles from the experimental data. The reduced quark multipoles were then fitted to a smooth curve. The fit results are shown by the shaded band in Fig. 1, where the band width accounts for the uncertainty of the measured amplitudes. The central values of the band can be written analytically as follows ($\mathbf{q}^2_{\rm EVF}<4{\rm GeV}^2$):

$$\tilde{e}^{11}=2.67+1.10\mathbf{q}^2_{\rm EVF}-0.21\mathbf{q}^4_{\rm EVF},$$

$$\tilde{m}^{11}=1.32-4.51\mathbf{q}^2_{\rm EVF}-0.10\mathbf{q}^4_{\rm EVF}, \qquad (17)$$

$$\tilde{m}^{12}=-1.34+9.20\mathbf{q}^2_{\rm EVF}-3.39\mathbf{q}^4_{\rm EVF}+0.34\mathbf{q}^6_{\rm EVF}.$$

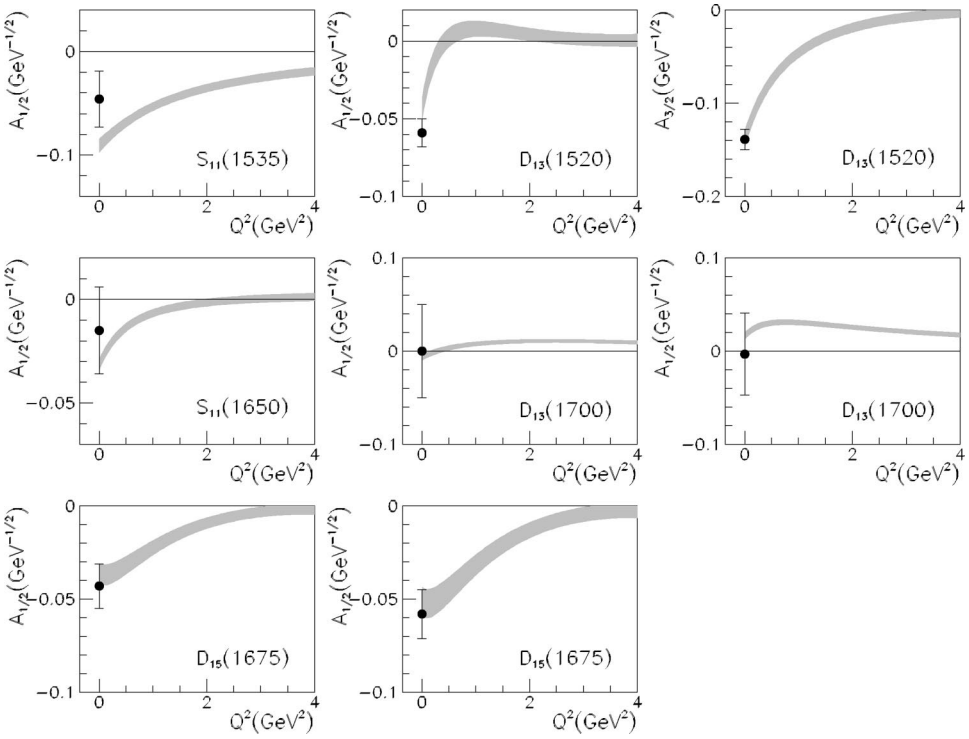


FIG. 4. Single quark model prediction for the [70, $1^-$] multiplet on the neutron. The SQTM predictions are shown by the shaded band in comparison with the experimental data. At $Q^2=0$ the full circle is the Particle Data Group estimate.

The $\mathbf{q}^6_{\mathrm{EVF}}$ term was added as the $\tilde{m}^{12}$ multipole shows a more complicated dependence on $\mathbf{q}_{\mathrm{EVF}}$ than the other multipoles. The quark multipole moments were then used to evaluate the SQTM prediction for all the states of the $[70,\ 1^-]$ multiplet. The results are shown in Figs. 2–4, where the SQTM predictions represented by the shaded bands are compared with the data. We do not show predictions for the $D_{15}(1675)$ on the proton as the state cannot mix and its amplitudes are predicted to be zero.

## VI. DISCUSSION

Comparison of the SQTM predictions with the data shows globally good agreement with the sparse data indicating that the model accounts for the main features of the excitations to the $[70,\ 1^-]$ for $Q^2 \leqslant 1\ \mathrm{GeV}^2$. We find that for states for which the signs of the amplitudes are known they are correctly predicted by the SQTM analysis. There is also quantitative agreement for most amplitudes at the photon point, and for amplitudes where good data on the $Q^2$ evolution are available, e.g., for the $S_{11}(1650)$ on the proton, excellent agreement is seen as well. The SQTM predictions, using a 31° mixing angle agree both in magnitude at the photon point, as well as with the $Q^2$ dependence. We take this as a confirmation of the adopted mixing angle, and as an indication that the SQTM works at a reasonable level for this state. Good agreement is also seen at the photon point for most other states. The poor quality of the electroproduction data for all other states does not allow drawing more definit conclusions.

In the case of the neutron states, both of the $D_{13}(1700)$ amplitudes, as well as the $D_{13}(1520)$ amplitudes, agree very well with the predicted ones at the photon point, while there are no electroproduction data available. Similarly, both $D_{15}(1675)$ amplitudes are in good agreement with the photoproduction data. This may be interpreted as a more direct confirmation of the SQTM assumptions as the latter state is not affected by mixing.

In the case of the $D_{33}(1700)$, the very large value of $A_{1/2}$ at $Q^2 = 0.5\ \mathrm{GeV}^2$ is likely unphysical, as it would produce a prominent enhancement in the inclusive cross section, which is not seen in the data. The $Q^2 = 1\ \mathrm{GeV}^2$ points are in disagreement with each other, while their average agrees with our prediction. A similar discrepancy between two data sets is seen for the $Q^2 = 1\ \mathrm{GeV}^2$ points of the $S_{31}(1620)$. Our prediction agrees with one of them. Given such systematic uncertainties in the electroproduction data we conclude that the SQTM predictions for the electromagnetic transition from the nucleon ground state to the $[70,\ 1^-]$ supermultiplet compare favorably with the available data. Obviously, much improved data are needed for more stringent tests of the model assumptions. It will be very interesting to see if and where the SQTM predictions break down. Such a breakdown could be due to nonquark contributions at lower $Q^2$, for example pion cloud effects. Such effects are currently being studied [36]. It may also indicate sizable multiquark transitions.

Additional experimental information on at least one state in the $[56,\ 2^+]$ supermultiplet, e.g., the $P_{13}(1720)$, is needed to uniquely extract the SQTM amplitudes for that supermultiplet. The main reason for the lack of data for states in the $[70,\ 1^-]$ and $[56,\ 2^+]$ supermultiplets is that many states couple only weakly to the $N\pi$ channel, the main source of information on resonance excitations. Most states have rather strong couplings to the $N\pi\pi$ channels. These channels are currently being studied in several experiments at JLab, GRAAL, and ELSA. Recent measurements of two-pion electroproduction at JLab may give access to several other states assigned to the $[56,\ 2^+]$ supermultiplet. This will allow more stringent tests of the SQTM predictions than are currently possible. No photoproduction or electroproduction data exist for any of the higher supermultiplets.


[1] N. Isgur and G. Karl, Phys. Rev. D **18**, 4187 (1978); **19**, 2653 (1979).
[2] L.Y. Glozman and D.O. Riska, Phys. Rep. **268**, 263 (1996).
[3] For a recent review see S. Capstick and W. Roberts, nucl-th/0008028.
[4] E. Pace, G. Salme, F. Cardarelli, and S. Simula, Nucl. Phys. **A666**, 33 (2000).
[5] M. Aiello *et al.*, J. Phys. G **24**, 753 (1998).
[6] Yu. A. Simonov, hep-ph/0205334.
[7] W. N. Cottingham and I. H. Dunbar, Z. Phys. C **2**, 41 (1979).
[8] A.J.G. Hey and J. Weyers, Phys. Lett. **48B**, 69 (1974).
[9] F.E. Close, *An Introduction Quarks and Partons* (Academic, London, 1979).
[10] R. Beck, R. Leukel, and A. Schmidt, A2 and TAPS Collaborations, Acta Phys. Pol. B **33**, 813 (2002).
[11] A. D'Angelo (unpublished).
[12] V.V. Frolov *et al.*, Phys. Rev. Lett. **82**, 45 (1999).
[13] C.S. Armstrong *et al.*, Phys. Rev. D **60**, 052004 (1999).
[14] R. Thompson *et al.*, CLAS Collaboration, Phys. Rev. Lett. **86**, 1702 (2001).
[15] K. Joo *et al.*, CLAS Collaboration, Phys. Rev. Lett. **88**, 122001 (2002).
[16] M. Dugger *et al.*, CLAS Collaboration (unpublished).
[17] M. Ripani *et al.*, CLAS Collaboration, hep-ex/0210054.
[18] M. Warns *et al.*, Phys. Rev. D **42**, 2215 (1990).
[19] S. Capstick, Phys. Rev. D **46**, 2864 (1992).
[20] L. A. Copley, G. Karl, and E. Obryk, Phys. Lett. **29B**, 117 (1969).
[21] R. Koniuk and N. Isgur, Phys. Rev. D **21**, 1868 (1980).
[22] R. G. Moorhouse, Phys. Rev. Lett. **16**, 771 (1966).
[23] N. Isgur and G. Karl, Phys. Lett. **72B**, 109 (1977).
[24] A.J.G. Hey, P.J. Litchfield, and R.J. Cashmore, Nucl. Phys. **B95**, 516 (1975).
[25] Particle Data Group, D. E. Groom *et al.*, Eur. Phys. J. C **15**, 1 (2000).
[26] I. Arai and J. Fujii (unpublished).
[27] N. Awaji *et al.* (unpublished); K. Fujii *et al.*, Nucl. Phys. **B197**, 365 (1982).
[28] R.L. Crawford and W.T. Morton, Nucl. Phys. **B211**, 1 (1983).

[29] W.J. Metcalf and R.L. Walker, in the Review of Particle Physics [Eur. Phys. J. C **15**, 1 (2000)].
[30] M. Rosenberg, Report No. BONN-IR-79-32 (unpublished); U. Beck *et al.*, Phys. Lett. **51B**, 103 (1974); H. Breuker *et al.*, *ibid.* **74B**, 409 (1978); H. Breuker *et al.*, Nucl. Phys. **B146**, 285 (1978); H. Breuker *et al.*, Z. Phys. C **13**, 113 (1982); H. Breuker *et al.*, *ibid.* **17**, 121 (1983).
[31] J.C. Alder *et al.*, Nucl. Phys. **B91**, 386 (1975); J.C. Alder *et al.*, *ibid.* **B99**, 1 (1975); J.C. Alder *et al.*, *ibid.* **B105**, 253 (1976); F.W. Brasse *et al.*, *ibid.* **B139**, 37 (1978); R. Haidan, DESY Report No. F21-79/02 (unpublished).
[32] W.J. Shuttleworth *et al.*, Nucl. Phys. **B45**, 428 (1972); P.S. Kummer *et al.*, Phys. Rev. Lett. **30**, 873 (1973); E. Evangelides *et al.*, Nucl. Phys. **B71**, 381 (1974); S. Hill, Ph.D. thesis, University of Manchester; A. Latham, Ph.D. thesis, University of Manchester; J. V. Morris *et al.*, Phys. Lett. **73B**, 495 (1978); J. V. Morris *et al.*, *ibid.* **86B**, 211 (1979); A. Latham *et al.*, Nucl. Phys. **B156**, 58 (1979); M. Davenport, Ph.D. thesis, University of Manchester; A. Latham *et al.*, Nucl. Phys. **B189**, 1 (1981); J. Wright *et al.*, *ibid.* **B181**, 403 (1981).
[33] F. Foster and G. Hughes, Rep. Prog. Phys. **46**, 1445 (1983).
[34] Ch. Gerhardt, Z. Phys. C **4**, 311 (1980).
[35] G. Krösen, Internal Report No. BONN-IR-83-3 (unpublished).
[36] D. Morel and S. Capstick, nucl-th/0204014 (unpublished).